Atomic structures and electrical resistivities of ternary liquid alloys

1997 J. Phys.: Condens. Matter 9 1393

(http://iopscience.iop.org/0953-8984/9/7/005)

J. Phys.: Condens. Matter **9** (1997) 1393–1406. Printed in the UK PII: S0953-8984(97)73715-9

Atomic structures and electrical resistivities of ternary liquid alloys

Z H Jin†, K Lu†, Z Q Hu† and H B Liu‡

† State Key Laboratory for Rapidly Solidified Non-equilibrium Alloys, Institute of Metal Research, Academia Sinica, Shengyang, 110015, People's Republic of China

‡ School of Materials Science and Engineering, Harbin Institute of Technology, Harbin, 150001, People's Republic of China

Received 16 April 1996, in final form 17 October 1996

Abstract. A self-consistent energy-independent non-local model pseudopotential theory has been developed for ternary alloys of simple metals for the first time. For K–Rb–Cs alloys, the partial structure factors are obtained by a solution of the standard Percus–Yevick equations for a ternary mixture of hard spheres. These partial structure factors are applied to calculate the electrical resistivities in the full concentration range of the alloy using the Ziman theory. Both the structure factors and the pseudopotential calculated form factors have been shown to be concentration sensitive. It has been shown that the electrical resistivities of the binary liquid alloys, such as K–Rb or K–Cs which exhibit nearly ideal structural behaviour, can be predicted to be in reasonable agreement with the experimental data. For ternary alloys, the calculated electrical resistivities vary smoothly with the concentration of each constituent, follow a well defined pattern in continuity and form a so-called 'electrical resistivity surface'. The results suggest that both the second-order non-local pseudopotential perturbation theory and the Ziman formalism are quite applicable in the prediction of the electrical resistivities of the multi-component alloys.

1. Introduction

The pseudopotential theory constructed from the first principles has been widely used in the prediction and interpretation of both the atomic and the electronic structures of simple metals and their binary alloys (for a review see, e.g., Hafner (1987) and Young (1992)). However, such investigations for multi-component simple metallic alloys are still relatively unexplored. In the early 1980s, a self-consistent energy-independent non-local model pseudopotential (EINMP) (Wang, Lai and So 1980, hereafter referred to as I, Wang and Lai 1980, hereafter referred to as II) was derived for use in the calculation of the electronic structure of the binary alloys of simple metals. The derived non-local pseudopotential contains a marked concentration dependence and has been successfully applied to the calculation of electronic transport coefficients of some alkali binary alloys and some Li-based polyvalent binary alloys. This has prompted us to consider further application of the derived pseudopotential to alloys containing three different simple metallic constituents.

The details of the calculation of the pair potentials that are parallel to the formula for binary alloys in EINMP theory are given in this paper for the first time. The K–Rb–Cs alloy systems have been chosen to be investigated as examples because they exhibit simple structural properties. For binary liquid alloys such as K–Rb, K–Cs and Rb–Cs, nearly ideal behaviour has been expected from both the experimental and the theoretical points of view

0953-8984/97/071393+14$19.50

(see Alblas *et al* (1981) and references therein). The electrical resistivities of some of those liquid binaries such as K–Rb and Na–Cs have also been well studied within the accuracy of the Ziman formalism by taking into account the non-local nature of the pseudopotentials (see e.g., Devlin *et al* (1973) and I). It has been shown that the Ziman-type theory can be applied successfully in the prediction of the electrical transport properties for simple binary alloy systems. However, a close examination of its applicability to multi-component systems is still needed.

It is well known that, for a random binary system, the three partial structure factors can only be derived uniquely from three diffraction experiments independently. For ternary alloys, generally speaking, six diffraction experiments are required, which can hardly be performed in laboratory. This forced us to rely upon results obtained from the solution of the well known Percus–Yevick equation for a model liquid consisting of hard spheres.

The rest of the article is organized as follows. In section 2 the EINMP has been extended to ternary alloy systems and the interatomic pair potentials for K–Rb–Cs alloys calculated; then the effective hard-sphere diameters and hence the partial structure factors have been determined. In section 3, these structure factors are used to calculate the electrical resistivities for pure K, Rb and Cs metals, binary K–Rb, Cs–Rb and K–Cs alloys and ternary K–Rb–Cs alloys. The influence of the form factors and structure factors on the electrical resistivities has been studied in comparison with the data experimentally available. The reliability of the second-order pseudopotential perturbation calculations, the hard-sphere partial structure factors and the applicability of the Ziman theory for ternary liquid alloys used have been checked. Conclusions are finally drawn in section 4.

2. Pair potentials and structure factors for ternary A–B–C alloys

2.1. Calculation of interatomic pair potentials

The numerical calculation of interatomic pair potentials $V_{ij}(R)$ for ternary A–B–C alloys can be performed in a similar manner to that for pure metals and their binary alloys (I and II). The pair potential $V_{ij}(R)$, i.e. $V_{AA}(R)$ between two A-type atoms, $V_{BB}(R)$ between two B-type atoms, $V_{CC}(R)$ between two C-type atoms, $V_{AB}(R)$ between A- and B-type atoms and $V_{AC}(R)$ between A- and C-type atoms, and $V_{BC}(R)$ between B- and C-type atoms, can be written as

$$V_{ij}(R)^* = Z_{eff,i}Z_{eff,j}R^{-1}\left(1-\pi^{-1}\int_0^\infty \mathrm{d}q[F_{i,j}(q)+F_{j,i}(q)]q^{-1}\sin(Rq)\right) \tag{1}$$

where $R = |\boldsymbol{R}_{\mu(j)} - \boldsymbol{R}_{\lambda(i)}|$, $\boldsymbol{R}_{\lambda(i)}$ is the ionic position vector for λth i-type (i = A, B, C or 1, 2, 3) atom in the system considered. $Z_{eff,i}$ is the effective valence and

$$Z_{eff,i}Z_{eff,j} = Z_iZ_j - \rho_{i,d}\rho_{j,d} \tag{2}$$

with Z_i and $\rho_{i,d}$ being the actual valence and depletion charge, respectively, of the i-type ion. $F_{i,j}(q)$ denotes the normalized energy wavenumber characteristic and takes the form

$$F_{i,j}(q) = -[\Omega_0 q^2/(2\pi Z_{eff,i}Z_{eff,j})](G_{i,j}(q)+\Delta G_{i,j}(q)+H_{i,j}(q)+\Delta H_{i,j}(q)) \tag{3}$$

in which Ω_0 is the mean atomic volume. $G_{i,j}(q)$, $\Delta G_{i,j}(q)$, $H_{i,j}(q)$ and $\Delta H_{i,j}(q)$ have the same form as defined by equations (2.12), (2.13), (2.17) and (2.18) in II for binary alloys. It is worth noting that, for ternary alloys, equation (3) contains a concentration dependence through quantities such as E_k^0 (the unperturbed eigenenergy) and N_k (renormalization constant of the pseudo-wavefunction) as appearing in $\rho_{i,d}$ and the screened potential involved in the form factors. Hence, with the presence of a third component, a self-consistent

calculation must be performed as for pure and binary alloys. In EINMP theory, the form factor $w_{i,q}^{EC}(\boldsymbol{k})$ can be written as

$$w_{i,q}^{EC}(\boldsymbol{k}) = w_{i,q}(\boldsymbol{k}) + \Delta w_i(\boldsymbol{q}) \tag{4}$$

where $w_{i,q}(\boldsymbol{k})$ is the form factor in which the electron–electron interaction is treated within the Hartree-type approximation and $\Delta w_i(\boldsymbol{q})$ denotes a correction due to the exchange and correlation effects of the valence electrons to $w_{i,q}(\boldsymbol{k})$ (see equation (2.9) of II for details). $E_{\boldsymbol{k}}^0$ can be converted into

$$E_{\boldsymbol{k}}^0 = \frac{k^2}{2} + \sum_{i=1}^{3} c_i N \langle \boldsymbol{k}|w_i^0(\boldsymbol{r})|\boldsymbol{k}\rangle = \sum_{i=1}^{3} c_i E_{i,\boldsymbol{k}}^0 \tag{5}$$

where $w_i^0(\boldsymbol{k})$ is the bare ionic pseudopotential given by equation (2.2) of Woo *et al* (1975) with $N = \sum_i N_i$ where N_i and c_i are the number and the concentration, respectively, of the i-type ions or atoms in the alloy under consideration. The depletion charge is of the form

$$\rho_{i,d} = \frac{\Omega_0}{\pi} \int_0^{k_F} \mathrm{d}\boldsymbol{k}\, m^*(k)\alpha_i(k)(k|N_{\boldsymbol{k}}|)^2 \tag{6}$$

where $m^*(k)$ is the first-order density-of-states effective mass for a valence electron in the alloy and takes the form

$$m^*(k) = \frac{m_1^*(k)m_2^*(k)m_3^*(k)}{c_1 m_2^*(k)m_3^*(k) + c_2 m_1^*(k)m_2^*(k) + c_3 m_1^*(k)m_2^*(k)} \tag{7}$$

with $m_i^*(k)$ being the first-order density-of-states effective mass for a valence electron in the pure metal consisting of the i-type ions (see equation (2.28) in I where the details of $\alpha_i(k)$ was also given). The normalization constant $N_{\boldsymbol{k}}$ is calculated to be

$$|N_{\boldsymbol{k}}|^2 = \frac{c_1 m_2^* m_3^* + c_2 m_1^* m_3^* + c_3 m_1^* m_2^*}{c_1 m_2^* m_3^* |N_{1,\boldsymbol{k}}|^{-2} + c_2 m_1^* m_3^* |N_{2,\boldsymbol{k}}|^{-2} + c_3 m_1^* m_2^* |N_{3,\boldsymbol{k}}|^{-2}} \tag{8}$$

for ternary alloys, with $|N_{1,\boldsymbol{k}}|^{-2}$ having the same meaning as equation (2.29) in I. The Fermi wavevector may be determined, as usual, from the equation

$$k_F^3 = 3\pi^2 \Omega_0^{-1} \sum_{i=1}^{3} c_i Z_i. \tag{9}$$

The formula for ternary alloys, such as (5), (7) and (8) derived here, can be converted to those forms for binaries if c_3 is set to zero. So they can be regarded as the unified form for A–B–C alloys in the full concentration range (including pure metal and binary alloy cases). In order to obtain the pair potentials of a ternary alloy according to equation (1) we have used firstly the EINMP as the bare pseudopotential for the ions in alloys and secondly the Ichimaru–Utsumi (1981) type of exchange–correlation factor in the calculation of the screened pseudopotentials.

For K–Rb–Cs ternary alloys, since no reliable experimental values of the atomic volumes Ω_0 are available to us, it has been assumed that Ω_0 changes linearly with the concentrations of K, Rb and Cs, i.e.

$$\Omega_0 = c_K \Omega_K + c_{Rb}\Omega_{Rb} + c_{Cs}\Omega_{Cs} \tag{10}$$

where Ω_K, Ω_{Rb} and Ω_{Cs} denote the atomic volumes of pure K, Rb and Cs, respectively, metals at the given temperature, and $c_K + c_{Rb} + c_{Cs} = 1$. Such calculated Ω_0 should contain no serious error in the fact that the maximum volume contractions are 1.0% for K–Cs and 5.7% for Na–Cs liquids (Alblas *et al* 1981).

The calculation of the pair potentials as described above has been performed for the ternary liquid K–Rb–Cs system at 100 °C and a number of different concentrations. The calculated pair potentials for $K_{0.6}Rb_{0.2}Cs_{0.2}$, $K_{0.4}Rb_{0.2}Cs_{0.4}$ and $K_{0.4}Rb_{0.4}Cs_{0.2}$ alloys are displayed in figure 1 as examples in comparing with those of pure K, Rb and Cs metals. The changes in the pair potentials due to alloying effects which merit emphasis have been summarized as follows.

(i) The first minimum of the pair potential of K–K shifts downwards with increasing Rb or Cs concentration, while that of Cs–Cs shifts upwards with increasing K or Rb concentration. Such a change is due mainly to the variation in the screening function with the mean electron density on alloying (see, e.g., Hafner (1987) and Young (1992)), i.e. the electron density of the K ion in alloys is smaller than that in pure K metal, while the electron density of Cs is larger than that in pure Cs metal.

(ii) The pair potentials for unlike pairs such as $V_{KRb}(R)$ and $V_{KCs}(R)$ and $V_{RbCs}(R)$ do not differ very much from the mean values of $\frac{1}{2}(V_{KK}(R) + V_{RbRb}(R))$, $\frac{1}{2}(V_{KK}(R) + V_{CsCs}(R))$ and $\frac{1}{2}(V_{RbRb}(R) + V_{CsCs}(R))$, respectively. This suggests that there is no significant non-additivity presented in the pair potentials. Hence, there should be no significant compound-forming or phase separation tendency for the system considered.

(iii) The above analyses disregard any variation in the pseudopotential of each component on alloying (see, e.g., Hafner (1987)). For some of the alkali-polyvalent alloys such as Li_4Pb, this effect may play a dominant role in the accurate calculation of the interatomic pair potentials. For the K–Rb–Cs alloys considered, which lack strong ordering tendencies, this effect is negligible.

(iv) Another effect which should be considered is that, for heavier alkali metals such as Rb and Cs, the d state has been presented and hence s–d mixing may occur in both the pure metals and their binary and ternary alloys. According to the argument of Li *et al* (1986, 1987), the s–d mixing effect can be simulated by slightly changing the effective core radius from the EINMP value R_l ($l = 0, 1, 2$), i.e. by replacing the parameter R_l in the EINMP by $R_l^M = R_l(1 + \delta)$, where δ is a small negative value. It has been found that the EINMP calculated form factors and the interatomic pair potentials are sensitive to δ. Such a modification can improve not only the thermodynamic and the structure results (Li *et al* 1986), but also the electrical resistivities calculated for alloys. This aspect will be further analysed in section 3.2.

In order to gain some further insight into the alloy properties on alloying, it is useful to have a close examination of the changes in the pseudopotential calculated on-Fermi-level form factors $w_{i,\boldsymbol{q}}^{EC}(k)$ and the depletion charges $\rho_{i,d}$ for ions in alloys with different concentrations. The results have been shown in figure 2 and figure 3 for some K–Rb–Cs alloy cases. It is found that the concentration dependence of both $w_{i,\boldsymbol{q}}^{EC}(k_F)$ and $\rho_{i,d}$ can be taken into account effectively in the self-consistent EINMP theory. We shall evaluate this concentration-dependent nature later. As for the depletion charge, the absolute value of $\rho_{i,d}$ for the electronegative ion (K in K–Rb and K–Cs or Rb in Rb–Cs) decreases with increasing non-electronegative ion concentration, while the absolute value of that for the non-electronegative ion (Rb in K–Rb or Cs in K–Cs and Rb–Cs) increases with increasing electronegative ion concentration. Figure 2 shows that for the ternary alloys the largest difference in the depletion charges occurs between the K and the Cs ions. This implies a charge-transfer mechanism which accounts for the electrical resistivity maximum in the alloys as discussed in II for alloys such as Na–Cs and Na–K, i.e. the partial localization of the valence electrons on the K ion (which always behaves as an electronegative ion) becomes larger in going from K–Rb to K–Cs alloy.

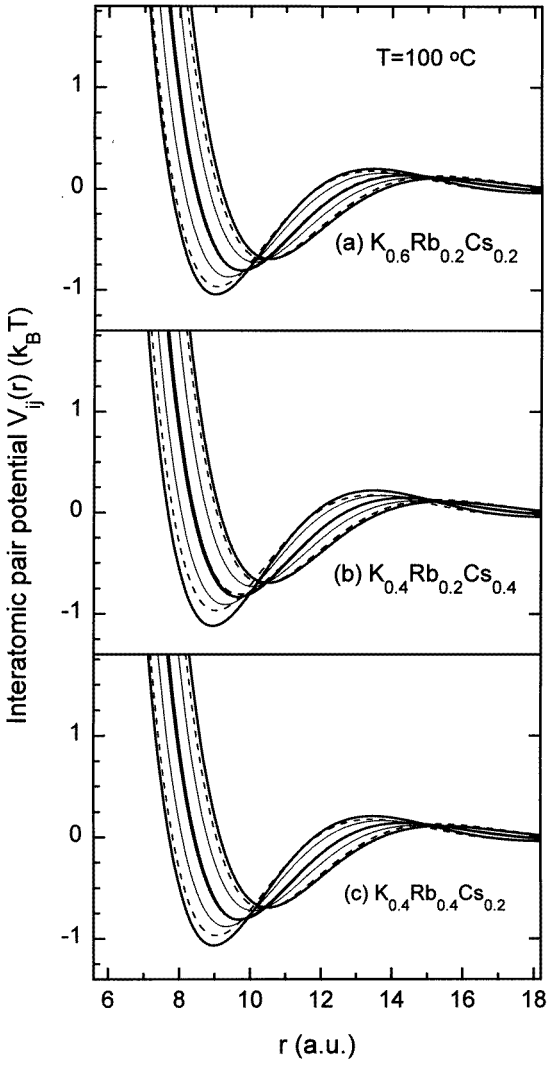

Figure 1. The EINMP calculated interatomic pair potentials for (a) $K_{0.6}Rb_{0.2}Cs_{0.2}$, (b) $K_{0.4}Rb_{0.2}Cs_{0.4}$ and (c) $K_{0.4}Rb_{0.4}Cs_{0.2}$ ternary alloys at 100 °C. From left to right; the thick curves represent the K–K, Rb–Rb and Cs–Cs interactions, the thin curves represent the K–Rb, K–Cs and Rb–Cs interactions, and the broken curves represent the interactions in pure K, Rb and Cs metals at 100 °C.

2.2. The hard-sphere partial structure factors

The expressions for the hard-sphere partial structure factors beyond the binary mixture in the Percus–Yevick approximation have been derived in the literature (Hoshino 1983) and are written in terms of the component concentration c_i, the hard-sphere diameter σ_i, and the partial packing density η_i. η_i takes the form

$$\eta_i = \pi c_i \sigma_i^3 / 6\Omega_0 \tag{11}$$

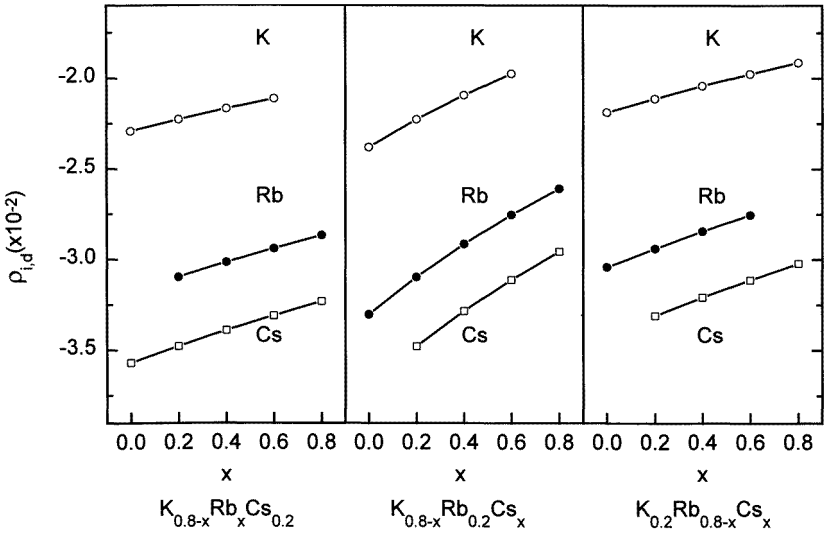

Figure 2. The depletion charges calculated from the EINMP theory for the ions in the ternary $K_{0.8-x}Rb_xCs_{0.2}$, $K_{0.8-x}Rb_{0.2}Cs_x$ and $K_{0.2}Rb_{0.8-x}Cs_x$ liquid alloys.

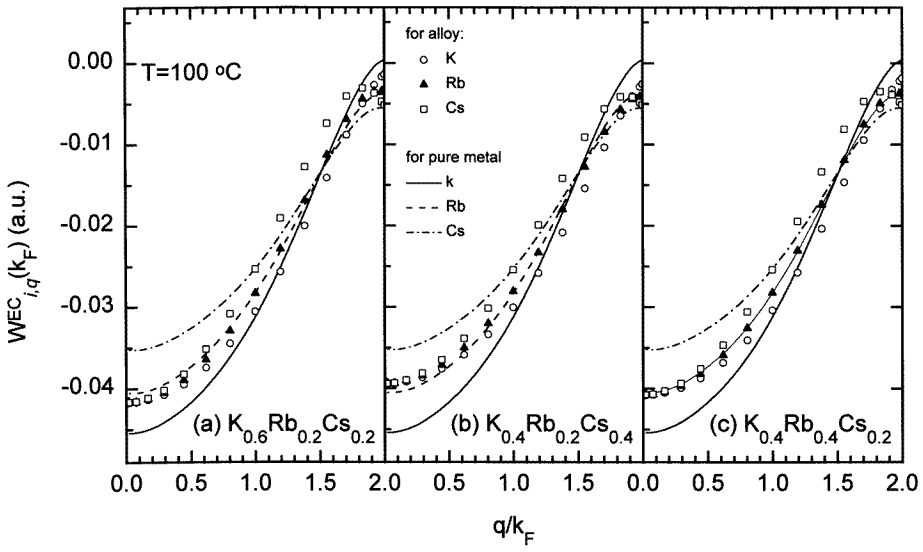

Figure 3. The EINMP calculated form factors for (a) $K_{0.6}Rb_{0.2}Cs_{0.2}$, (b) $K_{0.4}Rb_{0.2}Cs_{0.4}$ and (c) $K_{0.4}Rb_{0.4}Cs_{0.2}$ ternary alloys in comparison with those of pure K, Rb and Cs metals at 100 °C.

for a given ternary alloy. Once σ_1, σ_2 and σ_3 have been determined, the corresponding partial packing density and structure factors can be calculated. The values of σ_i can be determined as in II for binary alloys using a relation which was first suggested by Ashcroft and Langreth (1967b) and has been confirmed later by Hafner (1977) and Perry and Silbert

(1978), i.e.

$$V_{ii}(\sigma_i) = V_{ii}^{min} + \tfrac{3}{2}k_B T \tag{12}$$

where V_{ii}^{min} is the depth of the first minimum in the pair potential and k_B the Boltzmann constant. The thus determined σ_i-values are summarized in table 1, together with the mean atomic volumes, the total packing densities $\eta = \sum_i \eta_i$ for alloys at selected concentrations. It is worth noting that, for binary K–Rb, K–Cs and Rb–Cs liquid alloys, the concentration-dependent hard-sphere diameters for both the heavier ion and the lighter ion will be increased with increasing concentration of the lighter ion, all exhibiting a nearly linear behaviour. The resulting total packing density changes smoothly but deviates slightly from a linear relation with the alloy concentration. This is not a serious problem since we have assumed a linear concentration dependence of the mean atomic volumes in calculating the pair potentials and η_i. Finally, it should be noted that, since we have used a different exchange–correlation function in the pseudopotential calculation as in I or II, the σ_i-value may be a little different from those determined in I and II for pure metals and binary alloys.

Table 1. Values of atomic volume Ω_0 and the hard-sphere parameters σ_i and η for K–Rb–Cs alloys at various different concentrations c_i at 100 °C.

	c_K	c_{Rb}	c_{Cs}	Ω_0 (au)	σ_K (au)	σ_{Rb} (au)	σ_{Cs} (au)	η
K–Rb	1.0			535.0	7.589			0.428
	0.8	0.2		558.0	7.583	8.096		0.427
	0.6	0.4		581.0	7.571	8.090		0.426
	0.4	0.6		604.0	7.560	8.080		0.424
	0.2	0.8		627.0	7.554	8.069		0.423
		1.0		650.0		8.058		0.422
K–Cs	0.8		0.2	593.0	7.560		8.684	0.421
	0.6		0.4	651.0	7.531		8.664	0.415
	0.4		0.6	709.0	7.502		8.640	0.410
	0.2		0.8	767.0	7.471		8.614	0.406
			1.0	825.0			8.580	0.401
Rb–Cs		0.8	0.2	685.0		8.036	8.659	0.417
		0.6	0.4	720.0		8.014	8.639	0.412
		0.4	0.6	755.0		7.993	8.619	0.408
		0.2	0.8	790.0		7.977	8.600	0.404
K–Rb–Cs	0.6	0.2	0.2	616.0	7.554	8.069	8.684	0.420
	0.4	0.2	0.4	674.0	7.525	8.042	8.659	0.415
	0.4	0.4	0.2	639.0	7.542	8.063	8.674	0.419
	0.2	0.2	0.6	732.0	7.490	8.003	8.629	0.409
	0.2	0.4	0.4	697.0	7.513	8.025	8.649	0.413
	0.2	0.6	0.2	662.0	7.531	8.047	8.669	0.418

Having fixed σ_i and η_i, the structure factors can be calculated. The results have been displayed in figure 4 for pure K, Rb and Cs metals and in figure 5 for $K_{0.6}Rb_{0.2}Cs_{0.2}$, $K_{0.4}Rb_{0.2}Cs_{0.4}$ and $K_{0.4}Rb_{0.4}Cs_{0.2}$ ternary alloys at 100 °C. The results obtained for pure K, Rb and Cs are in good agreement with the experimental data (Waseda 1980) in the low-q ($q \leqslant 2k_F$) region as shown in the inset of figure 4. The concentration-dependent changes for each $a_{ij}(q)$ in ternary alloys are also clearly demonstrated. The reliability of the structure factors for binary and ternary alloys will be seen from their applications in the electrical resistivity calculations in the following sections.

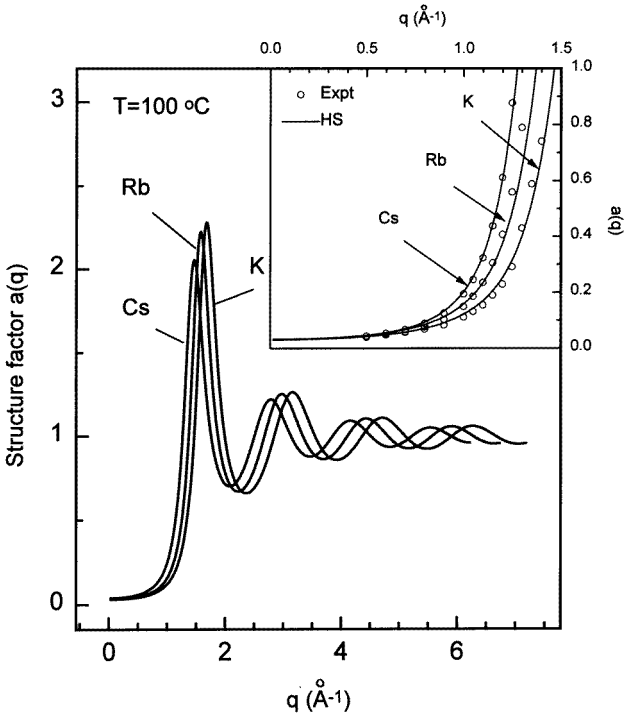

Figure 4. Hard-sphere structure factors for pure K, Rb and Cs metals at 100 °C. Comparisons with the experimental data (Waseda 1980) in the low-q regions ($q \leqslant 2k_F$) are displayed in the inset.

3. Electrical resistivities of K–Rb–Cs alloys

In this section, we apply the partial structure factors, as obtained in the preceding section, to calculate the electrical resistivities for K–Rb–Cs alloys at various different concentrations. The main purpose of this application is threefold:

(i) to examine the applicability of the partial structure factors as determined in section 2;
(ii) to study the concentration dependence of the electrical resistivities;
(iii) to check the reliability of the low-order pseudopotential perturbation theory and the Ziman theory for multi-component simple metallic alloys.

3.1. Expressions for the electrical resistivities of ternary alloys

According to I, II and Wang and So (1977), the electrical resistivity for alloy can be expressed as

$$\rho = [\langle m^*(k_F)\rangle |N_{\boldsymbol{k}_F}|^2]^2 \rho_f \tag{13}$$

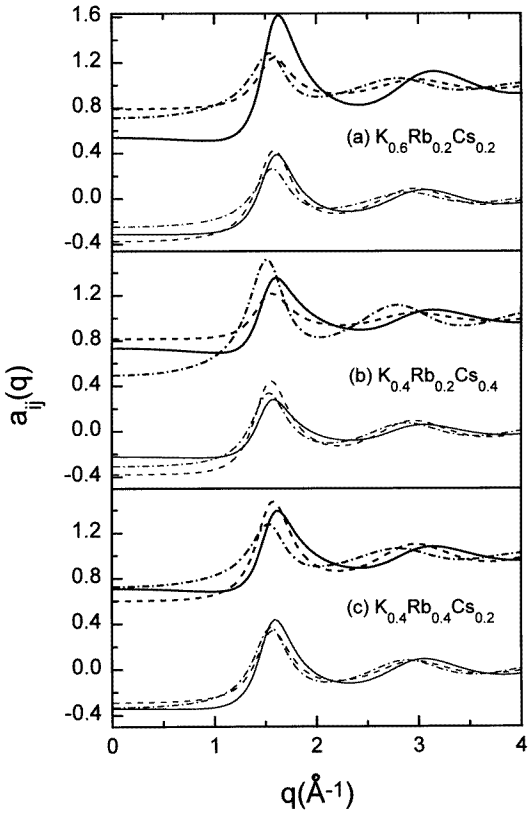

Figure 5. Partial structure factors calculated for (a) $K_{0.6}Rb_{0.2}Cs_{0.2}$, (b) $K_{0.4}Rb_{0.2}Cs_{0.4}$ and (c) $K_{0.4}Rb_{0.4}Cs_{0.2}$ ternary alloys at 100 °C. The upper three thick curves are as follows: ——, $a_{KK}(q)$; – – –, $a_{RbRb}(q)$; — · —, $a_{CsCs}(q)$. The lower three thin curves are as follows: ——, $a_{KRb}(q)$; – – – $a_{KCs}(q)$; — · — $a_{RbCs}(q)$.

where ρ_f is the electrical resistivity in the Ziman-type theory which is of the form (in atomic units system)

$$\rho_f = (3\pi\Omega_0/4k_f^6)\int_0^{2k_F} \mathrm{d}q\, q^3\Bigg(\sum_{i=1}^{3} c_i a_{ii}(q)|w_{i,\boldsymbol{q}}^{EC}(k_F)|^2 + 2(c_1c_2)^{1/2}a_{12}(q)w_{1,\boldsymbol{q}}^{EC}(k_F)w_{2,\boldsymbol{q}}^{EC}(k_F) + 2(c_1c_3)^{1/2}a_{13}(q)w_{1,\boldsymbol{q}}^{EC}(k_F)w_{3,\boldsymbol{q}}^{EC}(k_F) + 2(c_2c_3)^{1/2}a_{23}(q)w_{2,\boldsymbol{q}}^{EC}(k_F)w_{3,\boldsymbol{q}}^{EC}(k_F)\Bigg) \tag{14}$$

for ternary alloys. Herein $a_{ij}(q)$ is the Ashcroft–Langreth partial structure factors as determined in section 2, $\langle m^*(k_F)\rangle$ and $\boldsymbol{k}_F$ are the density-of-states effective mass $m^*(k_F)$ averaged over the Fermi surface and the Fermi wavevector, respectively; $w_{i,\boldsymbol{q}}^{EC}(k_F)$ is the on-Fermi-level form factor $w_{i,\boldsymbol{q}}^{EC}(k)$ calculated in a self-consistent manner with exchange–correlation effects included for the i-type ion in a ternary alloy A–B–C. In using the approximation as argued in II, if $\langle m^*(k_F)\rangle$ is approximated by the first-order density-of-states effective mass, then equation (13) becomes

$$\rho = [m_F^*(k_F)|N_{\boldsymbol{k}_F}|^2]^2\rho_f \tag{15}$$

where $m_F^*(k_F)$ and $|N_{\boldsymbol{k}_F}|^2$ can be calculated using equations (7) and (8) with k substituted by k_F. Equation (15) has been used in this work to calculate the electrical resistivities of K–Rb–Cs alloys at various different concentrations.

3.2. Electrical resistivities of pure alkali metals and their binary alloys

In order to check the accuracy of the theory and the hard-sphere structure factors used here, it is necessary to perform a comparison of the calculated and measured electrical resistivities for pure metals and their binary alloys. The theoretical results have been summarized in table 2. For pure metals K, Rb and Cs, the calculated electrical resistivities are 14.71 $\mu\Omega$ cm, 24.76 $\mu\Omega$ cm and 39.31 $\mu\Omega$ cm, respectively, at the corresponding melting points, compare favourably with the experimentally measured 13.1 $\mu\Omega$ cm, 22.0 $\mu\Omega$ cm and 36.0 $\mu\Omega$ cm. It has been found that, for the non-local pseudopotential calculated on-Fermi-level form factors, a kink at $q \approx 2k_F$ appears for Rb and Cs which leads to a larger departure from the zero value in comparison with that of K (cf figure 2). Since $a(q)$ increases abruptly as q approaches $2k_F$, the enhanced departure from the zero value of the form factor should contribute positively to the electrical resistivity for Rb or Cs. This also indicates that accurate form factors for ions in the alloys that exhibit a marked concentration dependence should be of extremely importance in yielding reasonable electrical resistivities.

Table 2. Theoretical values of $|N_{k_F}|^{-2}$, the valence-electron density-of-states effective mass $m_F^*(k_F)$ and the electrical resistivities ρ calculated for liquid K–Rb–Cs alloys at various different concentrations c_i at 100 °C.

	c_K	c_{Rb}	c_{Cs}	$\lvert N_{\boldsymbol{k}_F}\rvert^{-2}$	$m_F^*(k_F)$	$\rho(\mu\Omega$ cm)
K–Rb	1.0			0.9874	1.0301	17.09
	0.8	0.2		0.9866	1.0258	20.15
	0.6	0.4		0.9859	1.0213	22.85
	0.4	0.6		0.9851	1.0166	25.03
	0.2	0.8		0.9844	1.0118	26.64
		1.0		0.9837	1.0070	27.67
K–Cs	0.8		0.2	0.9866	1.0233	29.78
	0.6		0.4	0.9858	1.0154	39.88
	0.4		0.6	0.9850	1.0069	46.69
	0.2		0.8	0.9842	0.9982	49.77
			1.0	0.9834	0.9897	48.95
Rb–Cs	0.8		0.2	0.9836	1.0037	34.34
	0.6		0.4	0.9836	1.0003	39.88
	0.4		0.6	0.9835	0.9968	44.27
	0.2		0.8	0.9835	0.9932	47.33
K–Rb–Cs	0.6	0.2	0.2	0.9858	1.0185	31.80
	0.4	0.2	0.4	0.9850	1.0103	40.48
	0.4	0.4	0.2	0.9851	1.0136	33.23
	0.2	0.2	0.6	0.9842	1.0018	45.84
	0.2	0.4	0.4	0.9843	1.0053	40.55
	0.2	0.6	0.2	0.9843	1.0087	34.14

For binary alloys, K–Rb and K–Cs have been chosen as examples and the calculated results have been shown in figure 6 together with the experimental curves which were

taken from the results of Hennephof *et al* (1972, 1978). The results for K–Rb alloy are quite good. The K–Cs results, however, appear to be not quite as satisfactory. The discrepancy arises probably because we have used equation (15) instead of equation (13) to carry out the electrical resistivity calculations. The difference between the density-of-states effective mass $\langle m^*(k_F)\rangle$ and the first-order density-of-states effective mass $m^*(k_F)$ has been neglected. It has been argued in II that $m^*(k_F)$ does not contain a positive contribution from the partial localization of the valence electron on the electronegative ions; hence, equation (15) will lead to a underestimation of ρ calculated for an alloy such as K–Cs. On the other hand, the partial localization of the valence electron due to the s–d mixing effects with the presence of the heavier ion Cs may also lead to an increase in the electrical resistivities of the alloy system. Since it is rather difficult to calculate the higher-order contributions involved in $\langle m^*(k_F)\rangle$, we shall evaluate the above-mentioned two kinds of valence-electron-localization mechanism in a similar manner by modifying the core radius of the EINMP according to the suggestions given by point (iv) in section 2.1. This can be done by assuming that, for each component i, the δ_i-value will be in a linear relation to the concentration and increase as c_i is decreased. The largest $|\delta|$ is 0.018 for the K ion and 0.03 for Cs. The final result thus calculated for K–Cs is also illustrated in figure 6 and proves to be an excellent improvement. It is worth noting that, under such modifications, both σ_i and $w_{i,q}^{EC}(k)$ will be changed systematically and both contribute positively (similarly in magnitude) to the final ρ-value. Since the goal of this paper is not how to obtain good numerical results, the details of the related calculations will be published in a separate paper and the following results for K–Rb–Cs alloys (see also table 2) do not contain such modifications.

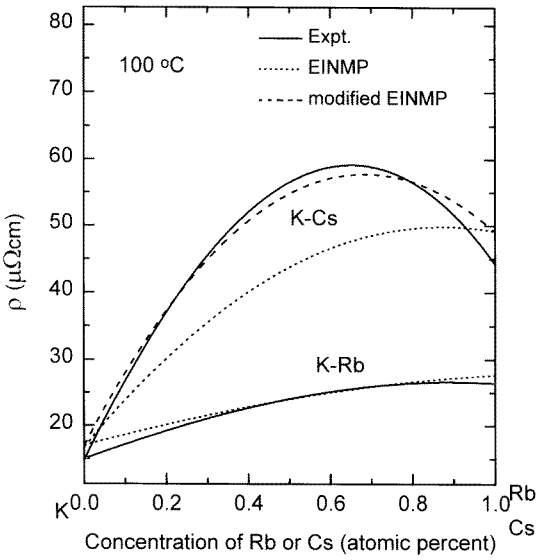

Figure 6. Electrical resistivities of liquid K–Rb and K–Cs alloys at 100 °C. ——, experimental results (Hennephof *et al* 1972, 1978); - - - -, EINMP results; – – –, modified EINMP results.

Besides the points mentioned above, the structural properties of K–Cs have been considered. It has already been mentioned that this alloy system exhibits nearly ideal mixing behaviour (we believe that the same will be true for K–Rb and Rb-Cs alloys). This can be

studied by looking at the Bathia–Thornton (1970) partial structure factors and specifically the long-wavelength limit of the concentration–concentration partial structure factor $S_{cc}(0)$. As figure 7 shows, the resulting $S_{cc}(0)$ of the hard-sphere model coincides with the values of $c(1-c)$ predicted according to the ideal-solution model, which does not differ very much from the experimental results (Devlin *et al* 1973). Hence, we may conclude that the electrical resistivity maximum does not necessarily have a close relationship to the possible existence of the chemical ordering or phase separation tendencies in the liquid structures, at least for the K–Cs alloy considered at 100 °C.

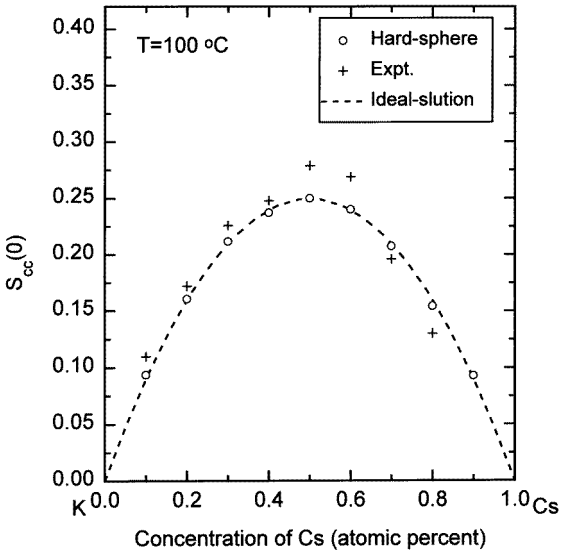

Figure 7. The values of $S_{cc}(0)$ for liquid K–Cs alloys at 100 °C as a function of the potassium concentration: – – –, ideal solution, $S_{cc}(0) = c(1-c)$; ○ , hard-sphere model; +, experimental x-ray results (Alblas *et al* 1981).

3.3. Electrical resistivities of ternary alloys

The calculation of the electrical resistivities as described above is applied to the K–Rb–Cs alloys at 100 °C. The results thus calculated are summarized in table 2 for some alloys at selected concentrations. The electrical resistivity of the alloys, generally speaking, increases substantially from K-rich alloys to Rb-rich alloys and to Cs-rich alloys. However, such an increase is by no means linear if weighted by concentration in using the values of pure metals. The features worth noting are as follows.

(i) There is a pronounced maximum in the binary K–Cs alloys which is located at the higher atomic concentrations of the heavier element, i.e. at about 60–70 at% Cs. Such a maximum also appears for ternary K–Rb–Cs alloys if the concentration of Rb is set to, for example, 20 at%.

(ii) There is no maximum for K–Rb and Rb–Cs binary alloys, but the calculated results indicate that the departure from the mean electrical resistivity $c_1\rho_1 + (1-c_1)\rho$ can be as large as 8% of the mean value. In fact, this has already led to a flat top in the ρ-values for Rb–Cs alloy.

(iii) The electrical resistivities calculated for ternary K–Rb–Cs alloys (including binaries and pure K, Rb and Cs metals) change smoothly with the concentration of each component and, thus, form a well defined 'electrical resistivity surface' at 100 °C. This can be seen even more clearly when they are drawn in the three-dimensional space using the equilateral composition triangle, as shown in figure 8.

Points (i) and (ii) can be understood by recalling that the localization of the valence electrons on the electronegative component in the K–Cs alloy is larger than that in K–Rb and Rb–Cs alloys, as argued in I, II and section 3.2 of this paper. Such a charge-transfer mechanism, which is concentration dependent, can contribute both to the pseudopotential calculated on-Fermi-level form factors (cf figure 3) and to the pair potential-determined σ_i and therefore the partial structure factors $a_{ij}(q)$ (cf figure 4), to yield systematic changes in ρ as noted above. Since changes in $m_F^*(k_F)$ and $|N_{\boldsymbol{k}_F}|^2$-values due to alloying (cf table 2) are not large enough to cause a significant change in ρ at certain concentrations as noted in the above points (i) and (ii), they contribute only an overall correction to the calculated electrical resistivities when including full non-locality in the pseudopotential calculation. Point (iii) is direct verification of the validity of the self-consistent non-local pseudopotential calculation for ternary alloy used here; it also confirms that the σ_i-values and the calculated partial structure factors of the hard-sphere model within the Percus–Yevick approximation are reasonable to apply to calculate the electrical resistivities for ternary liquid alloys within the Ziman formalism.

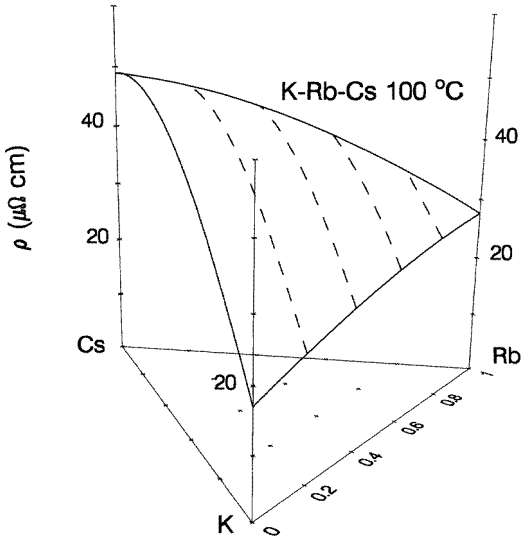

Figure 8. Theoretical 'electrical resistivity surface' of the K–Rb–Cs alloys at 100 °C.

4. Conclusion

In this paper, for the first time, the EINMP theory that was formerly developed for binary alloys of simple metals has been generalized self-consistently to ternary alloy systems to calculate the interatomic pair potentials. From the calculated pair potentials for the alkali K–Rb–Cs alloys, the hard-sphere diameters of each component can be determined and the

partial structure factors are obtained by a solution of the Percus–Yevick equations for a ternary mixture of hard spheres. These partial structure factors and the form factors as employed in the computation of the pair potentials were used to calculate the electrical resistivities for K–Rb–Cs alloys at 100 °C within the Ziman formalism.

From the calculated results we concluded the following.

(i) The calculated electrical resistivities of pure metals and binary alloys are in good agreement with the experimental data, within the accuracy of the Ziman formalism.

(ii) The partial localization of the electrons on the electronegative component in the alloy can be used in the interpretation of the electrical resistivity maximum presented in K–Rb–Cs liquid alloys which exhibit a nearly ideal structural behaviour.

(iii) For ternary alloys in the full concentration range, the calculated electrical resistivities vary smoothly with the changing composition of each alloy component, follow a well defined pattern in continuity and form a so-called 'electrical resistivity surface'.

(iv) Both the second-order non-local pseudopotential perturbation theory and the Ziman formalism have proved to be quite applicable in the prediction of the electrical resistivities of the multi-components alloys.

Acknowledgments

One of the authors (Z H Jin) is grateful to Dr S Wang, University of Waterloo, Canada, for his kind guidance in initiating this work. Financial support from the National Science Foundation of China is acknowledged.

References

Alblas B P, Van der Lugt W, Mensies O and Van Dijk C 1981 *Physica* B **106** 22–32
Ashcroft N W and Langreth D C 1967a *Phys. Rev.* **156** 685–92
——1967b *Phys. Rev.* **159** 500–10
Bathia A B and Thornton D E 1970 *Phys. Rev.* B **2** 3004–12
Devlin J F, Leenstra M R and Van der Lugt W 1973 *Physica* **66** 593–600
Hafner J 1977 *Phys. Rev.* A **16** 351–64
——1987 *From Hamiltonians to Phase Diagrams* (Berlin: Springer)
Hennephof J, Van der Lugt W, Wright G W and Mariën T 1972 *Physica* **61** 146–51
Hennephof J, Van der Marel C and Van der Lugt W 1978 *Physica* B **94** 101–4
Hoshino K 1983 *J. Phys. F: Met. Phys.* **13** 1981–92
Ichimaru S and Utsumi K 1981 *Phys. Rev.* B **24** 7385–9
Li D H, Li X R and Wang S 1986 *J. Phys. F: Met. Phys.* **16** 309–21
Li D H, Moore R A and Wang S 1987 *J. Phys. F: Met. Phys.* **16** 2007–15
Perry B N and Silbert M 1978 *J. Phys. C: Solid State Phys.* **11** 4907–20
Wang S and Lai S K 1980 *J. Phys. F: Met. Phys.* **10** 2717–37
Wang S, Lai S K and So C B 1980 *J. Phys. F: Met. Phys.* **10** 445–59
Wang S and So C B 1977 *J. Phys. F: Met. Phys.* **7** 1439–52
Waseda Y 1980 *Structure of Non-crystalline Materials* (New York: McGraw-Hill)
Woo C H, Wang S and Matsuura M 1975 *J. Phys. F: Met. Phys.* **5** 1836–48
Young W H 1992 *Rep. Prog. Phys.* **55** 1769–853